

Synchronization in coupled chaotic oscillators with a no-flux boundary condition

Wenyuan Liu, Jinghua Xiao, and Junzhong Yang*

School of Science, Beijing University of Posts and Telecommunications, 100088 Beijing, China

(Received 5 March 2004; published 20 December 2004)

We investigate the synchronization of coupled chaotic oscillators with a no-flux boundary condition. We find that the spectrum of the coupling matrix is divided into two parts, the isolated part with a zero eigenvalue and the continuous one with the other $N-1$ eigenvalues falling onto a line. Based on the eigenvalue analysis, the stability of the synchronization in a coupled Lorenz system is explored thoroughly in the parameter space of the size of the system, the diffusion, and gradient coupling constants.

DOI: 10.1103/PhysRevE.70.066211

PACS number(s): 05.45.Xt

Since Pecora and Carroll's pioneering work in 1990 [1], chaos synchronization has been a hot spot in nonlinear science. Especially, chaos synchronization in coupled chaotic oscillators has drawn lots of attention due to the fact that the coupled oscillators is a discrete version of a reaction-diffusion system widely found in physics, chemistry, biology, and social society. Numbers of phenomena have been observed and different kinds of synchronization, phase synchronization [2,3], generalized synchronization [4,5], and complete synchronization [6,7], have been classified according to the extent of synchronization among the elements in systems. In complete synchronization, the stability theories of the synchronous chaos have been proposed [8–10] and the bifurcation of the synchronous chaos has also been studied thoroughly [11–14]. However, most of the work is done on periodic boundary condition. Though no-flux boundary condition is more often seen in real systems, synchronization in those systems has not been paid enough attention [15–18].

Let us consider a very popular system of N identical coupled nonlinear oscillators with nearest coupling,

$$\begin{aligned} \dot{u}_j &= f(u_j) + (\epsilon - r)\Gamma(u_{j+1} - u_j) + (\epsilon + r)\Gamma(u_{j-1} - u_j), \\ j &= 1, 2, \dots, N, \end{aligned} \quad (1)$$

where $u_j \in \mathbb{R}^n$. The function f is nonlinear and capable of exhibiting chaotic solution, ϵ and r are the dimensionless scalar diffusive and gradient coupling parameter, respectively, and Γ is an $n \times n$ constant matrix linking coupled variables. Generally, there are four situations depending on the type of boundary condition and whether or not there exists a gradient coupling term: (i) a system with periodic boundary condition (PBC) and no gradient coupling term; (ii) a system with PBC and a gradient coupling term; (iii) a system with no-flux boundary condition (NBC) and no gradient coupling term; (iv) a system with NBC and a gradient coupling term. In this paper, we will use the eigenvalue analysis [8,9] to investigate complete synchronization in the latter two cases and compare it with that of the former two.

The synchronous chaos falls onto the synchronous manifold and is represented as $u_1(t) = u_2(t) = \dots = u_N(t) = s(t)$, where $\dot{s}(t) = f(s(t))$. Its stability can be analyzed by setting $u_j = s(t) + \eta_j$. By linearizing Eq. (1) at the synchronous chaos $s(t)$, we have

$$\dot{\eta} = [Df(s)I + B\Gamma]\eta, \quad (2)$$

where $Df(s)$ is the Jacobian of f on $s(t)$, $\eta = (\eta_1, \eta_2, \dots, \eta_N)^T$, I is an $N \times N$ unit matrix, and B is an $N \times N$ coupling matrix. Expanding η over the eigenfunctions of B , we get

$$\dot{\delta}_k = [Df(s)I + \lambda_k \Gamma]\delta_k, \quad (3)$$

where $\delta_k \in \mathbb{R}^n$ and λ_k is the eigenvalue of the coupling matrix B . Now we have reduced the N -site coupled equations (1) to much simpler N independent modified one-site equations, and then the stability problem of the synchronous chaos can be analyzed in n -dimensional space rather than in $(N \times n)$ -dimensional space.

The significance of Eq. (3) is that the stability problem of Eqs. (1) can be separated into two independent problems: one is to analyze the stable regions of Eq. (3), this depends on the single-site parameters only [such as the reference orbit $s(t)$, the Jacobian $Df(s)$, and the inner linking matrix Γ], and is independent of the coupling matrix B and the system size N ; the other is to analyze the eigenvalue distribution of the coupling matrix B , that depends on the diffusive and gradient couplings, the size of system only, and the boundary condition, and is independent of the inner dynamics [including $s(t)$, $Df(s)$, and Γ]. Both problems can be solved easily and the solutions of these two problems can be put together to entirely answer the complicated stability problem of Eqs. (1).

For each λ_k , Eq. (3) provides n Lyapunov exponents along the synchronous orbit $s(t)$. The maximum Lyapunov exponent of Eqs. (3) is denoted by β . By treating λ_k as a controllable parameter (we omit the subscript for λ_k below), the criterion that maximum Lyapunov exponent of Eq. (3) should be negative, $\beta < \beta_c \equiv 0$, provides the stability boundary for the synchronous orbit $s(t)$ in the $\text{Re}(-\lambda)$ - $\text{Im}(\lambda)$ parameter plane (note that λ can be complex for asymmetric couplings, $r \neq 0$). We term the stability boundary as critical curve which divides the complex plane of λ into stable ($\beta < 0$) and unstable regions ($\beta > 0$) [see the V-shaped curve in

*Author to whom correspondence should be addressed. Electronic address: jzyang@bupt.edu.cn

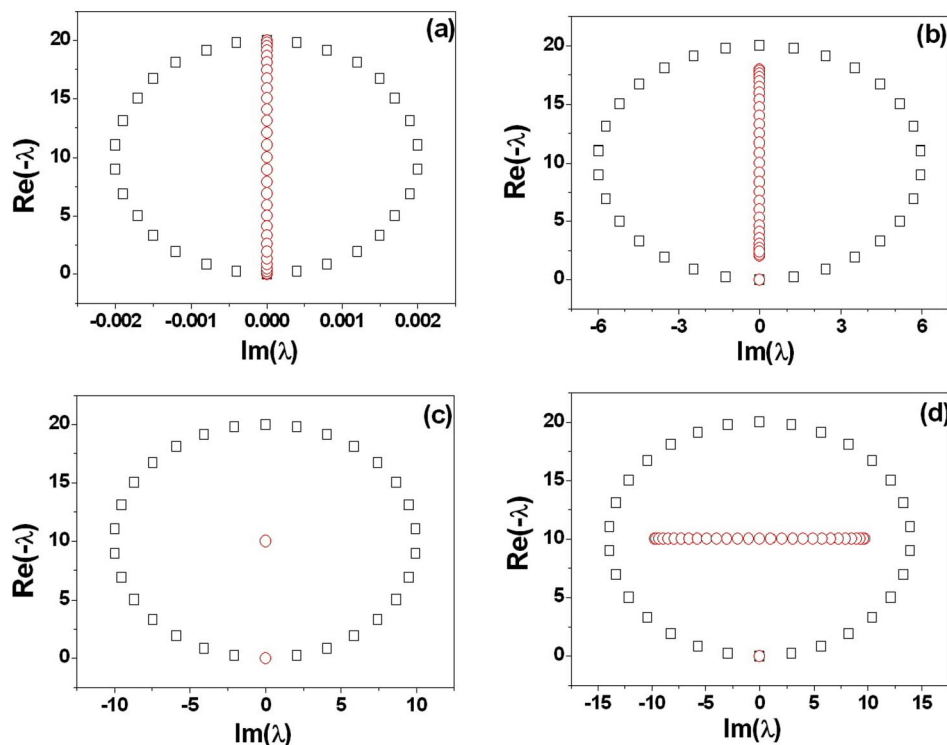


FIG. 1. (Color online) The eigenvalue distributions of coupling matrices for PBC (open squares) and NBC (open circles) systems, $N=30$. (a) $\epsilon=5$, $r=0.001$ ($\epsilon > r$); (b) $\epsilon=5$, $r=3$ ($\epsilon > r$); (c) $\epsilon=r=5$; (d) $\epsilon=5$, $r=7$ ($\epsilon < r$).

Figs. 2(a) and 3(a)]. Once the critical curve is given, the stability of the synchronous chaos can be determined by examining whether eigenvalues of coupling matrix B enter into the unstable region in $\text{Re}(-\lambda)$ - $\text{Im}(-\lambda)$ plane. If there are other eigenvalues falling into the unstable region except for one zero eigenvalue, the synchronous orbit $s(t)$ is unstable with respect to transversal perturbations.

In the nearest coupling scheme, the coupling matrices B for PBC and NBC are

$$B = \begin{pmatrix} -2\epsilon & \epsilon+r & & \epsilon-r \\ \epsilon-r & -2\epsilon & \epsilon+r & 0 \\ & \dots & \dots & \dots \\ & & \epsilon-r & -2\epsilon & \epsilon+r \\ \epsilon+r & & & \epsilon-r & -2\epsilon \end{pmatrix} \quad (4)$$

and

$$B = \begin{pmatrix} -(\epsilon+r) & \epsilon+r & & & \\ \epsilon-r & -2\epsilon & \epsilon+r & & \\ & \dots & \dots & \dots & \\ & & \epsilon-r & -2\epsilon & \epsilon+r \\ & & & \epsilon-r & -(\epsilon-r) \end{pmatrix}, \quad (5)$$

respectively.

In the PBC case, the system has a shift-invariant symmetry [15] and the eigenvalues of the matrix B are given in Refs. [8,9] as

$$\lambda_k = 2\epsilon[-1 + \cos(2\pi k/N)] + i2r \sin(2\pi k/N),$$

$$k = 0, 1, \dots, N-1. \quad (6)$$

The real and imaginary part of the eigenvalues satisfy the elliptic relation and all eigenvalues distribute uniformly on an ellipse, as shown in Fig. 1. It is clear that the spectrum of the matrix B is continuous in the limit of $N \rightarrow \infty$. With the number of the oscillators increasing, the density of the eigenvalues on the ellipse increases linearly. For the no-flux boundary condition, the eigenvalues of the coupling matrix B are obtained as

$$\lambda_k = \begin{cases} -2\epsilon + 2\sqrt{\epsilon^2 - r^2} \cos\left(\frac{\pi k}{N}\right), & k = 1, \dots, N-1 \\ 0, & k = 0. \end{cases} \quad (7)$$

Contrary to the PBC case, the system with no-flux boundary condition does not have the shift-invariant symmetry. However, if there is no gradient coupling, the system with NBC (represented by $\{1, 2, \dots, N\}$) can be created from a system with PBC by doubling the size of the PBC system (represented by $\{1, 2, \dots, N, N+1, \dots, 2N\}$) [15,19,20]. If we force the $N+1$ th oscillator to be the same as the N th and the $2N$ th equal to the 1st, the doubled system becomes $\{1, 2, \dots, N, N, \dots, 2, 1\}$ and the dynamics of the first N oscillators follows the equations described by the coupling matrix in Eq. (5). Utilizing the shift invariant symmetry in the doubled system with PBC, the eigenvalues of the coupling matrix in Eq. (5) can be obtained as $\lambda_k = -4\epsilon \sin^2(\pi k/2N)$, $k=0, 1, \dots, N-1$ [15]. Setting $r=0$ in Eq. (7), we recover the results in Ref. [15]. Unfortunately, the treatment above is not applicable to the system with NBC when the gradient coupling is present ($r \neq 0$). The doubled system $\{1, 2, \dots, N, N, \dots, 2, 1\}$ does not have a shift-invariant sym-

metry because the directionality of the gradient coupling makes the conjunctions between the subsystems $\{1, 2, \dots, N\}$ and $\{N, \dots, 2, 1\}$ be source and sink of the flow. Actually the absence of the connection between systems with PBC and with NBC when gradient coupling $r \neq 0$ is evidenced by the formulas in Eqs. (6) and (7). To make it clear, we use `Matlab` to calculate the eigenvalues of B directly. The eigenvalue distributions in the $\text{Re}(-\lambda)\text{-Im}(\lambda)$ plane for different r under PBC and NBC cases are shown in Figs. 1(a)–1(d) where $N = 30$ and $\epsilon = 5$. From these figures, we find that the distribution of the eigenvalues in the NBC case is quite different from the PBC case. First of all, the spectrum of the matrix B is divided into two parts. One is an isolated part containing only $\lambda = 0$ which accounts for the synchronous state, the other is a continuous part which includes the other $N - 1$ eigenvalues. Second, the eigenvalues in the continuous part for the NBC case fall onto not an ellipse but a line (we call it the distribution line) whose orientation is determined by the relative strength of ϵ and r . When $r < \epsilon$, the imaginary parts of the eigenvalues are zero, the distribution line is on the real axis of the complex λ_k plane. The situation is unchanged even when the gradient coupling is extremely small, for example $r/\epsilon = 0.0002$: the eigenvalues for PBC fall onto an ellipse while those for NBC still onto a line [Fig. 1(a)]. The results in Fig. 1(a) indicate that the connection between a PBC system with doubled size and an NBC system when $r = 0$ is rather special, not a universal property. Moreover, for $r > \epsilon$, the real parts of the eigenvalues equal to $-\epsilon$ and the line is parallel to the imaginary axis. For a special case $r = \epsilon$, the continuous part for the NBC case collapses onto a single point, that is, the only eigenvalue in the continuous part is $(N - 1)$ -fold degenerate. Actually, $r = \epsilon$ with NBC corresponds to a one-way coupled open system [21] where the dynamics at the upper stream is independent of other sites downstream. As a result, the synchronization condition of the whole NBC system is the same as that for a driver-slaver system [1] where $N = 2$. However, the dynamics of the one-way coupled PBC system is controlled by the collective behaviors of all sites [22] and the eigenvalues of B still distribute onto a certain ellipse.

Now consider a specific system. We choose the Lorenz oscillator as the constituent element. The Lorenz oscillator is described by

$$\begin{cases} \dot{x} = \sigma(y - x) \\ \dot{y} = \rho x - y - xz \\ \dot{z} = xy - z, \end{cases} \quad (8)$$

where $\sigma = 10$ and $\rho = 28$. Under these parameters the dynamics of the single oscillator is chaotic. For the choice of

$$\Gamma = \begin{pmatrix} 0 & 0 & 0 \\ 1 & 0 & 0 \\ 0 & 0 & 0 \end{pmatrix},$$

the critical curve in the λ_k complex plane is of “V” shape as the solid line shown in Fig. 2(a). The necessary and sufficient condition for synchronization is that all the nonzero eigenvalues of the matrix B locate above the critical curve. $\epsilon, r,$

and N are controllable during the investigation of the stability of the synchronous chaos. First, we vary the gradient coupling constant r while keeping N and ϵ unchanged. From Eq. (7), we know that the length of the vertical distribution line decreases when r increases from 0. Then above $r = \epsilon$ where the eigenvalue is $(N - 1)$ -fold degenerate, the line changes its orientation to be horizontal and the length of the line increases with r . In the PBC case, the only effect of r is to desynchronize the system with V-type critical curve. However, in the case of NBC, r may induce synchronization. Figure 2 shows the simulation results for $N = 20$ and $\epsilon = 5$. In Fig. 2(a), we plot eigenvalues for different r in the $\text{Re}(-\lambda)\text{-Im}(\lambda)$ plane. The distribution line is vertical when $r = 2$. We can find that some eigenvalues are below the critical curve, which indicates that the synchronous chaos is unstable. When r increases, the length of the distribution line is shortened and the eigenvalues on the line move toward the midpoint so that the number of the eigenvalues below the critical curve decreases. Especially, when $r = 4.5$, the length of the line is so short that all eigenvalues in the continuous spectrum enter the stable region. After crossing $r = \epsilon = 5$, the orientation of the distribution line becomes horizontal. For example, when $r = 5.5$, $N - 1$ eigenvalues are all in the stable region. Further increasing r , the length of the line becomes longer and longer. Eventually some eigenvalues enter the unstable region again and synchronization is destroyed. Figure 2(b) shows the first four largest Lyapunov exponents of the coupled system versus r . We can find the transitions from desynchronization to synchronization for small r and the reverse process for large r , respectively. Synchronization is realized when r is around ϵ where there is only one positive Lyapunov exponent. Such transitions are also seen in Figs. 2(c)–2(f) where the fluctuations of x ,

$$\sigma = \sqrt{\frac{\sum (x_i - \bar{x}_i)^2}{N(N - 1)}}, \quad \bar{x}_i = \frac{\sum x_i}{N}, \quad (9)$$

are presented for different r .

In the following we investigate the effect of ϵ on the synchronization of the system. Let $N = 14$ and $r = 5$, we plot the eigenvalues for different ϵ on the $\text{Re}(-\lambda)\text{-Im}(\lambda)$ plane in Fig. 3(a). Several points from Fig. 3(a) can be drawn: (i) For small ϵ , the distribution line is horizontal. When ϵ increases from zero, the line is shortened at the same time it moves away from the imaginary axis. There exists a certain ϵ_0 , below which the distribution line does not intersect the critical curve and the synchronization is not possible whatever r is. When ϵ is larger than ϵ_0 , so that the synchronization could be realized by varying r according to the discussion above. (ii) For intermediate ϵ , once another critical value ϵ_1 is passed the horizontal line shrinks completely into the stable region, the synchronous chaos is stable. Still within this stable region, the distribution line becomes vertical after collapsing onto one point. (iii) A third critical diffusion coupling ϵ_2 could be found, above which the length of the line becomes long enough that its lower part moves down across the critical curve. The existence of ϵ_2 signals the desynchronization of the system. (iv) From Eq. (7), we know that ϵ not only changes the length of the distribution line but also changes

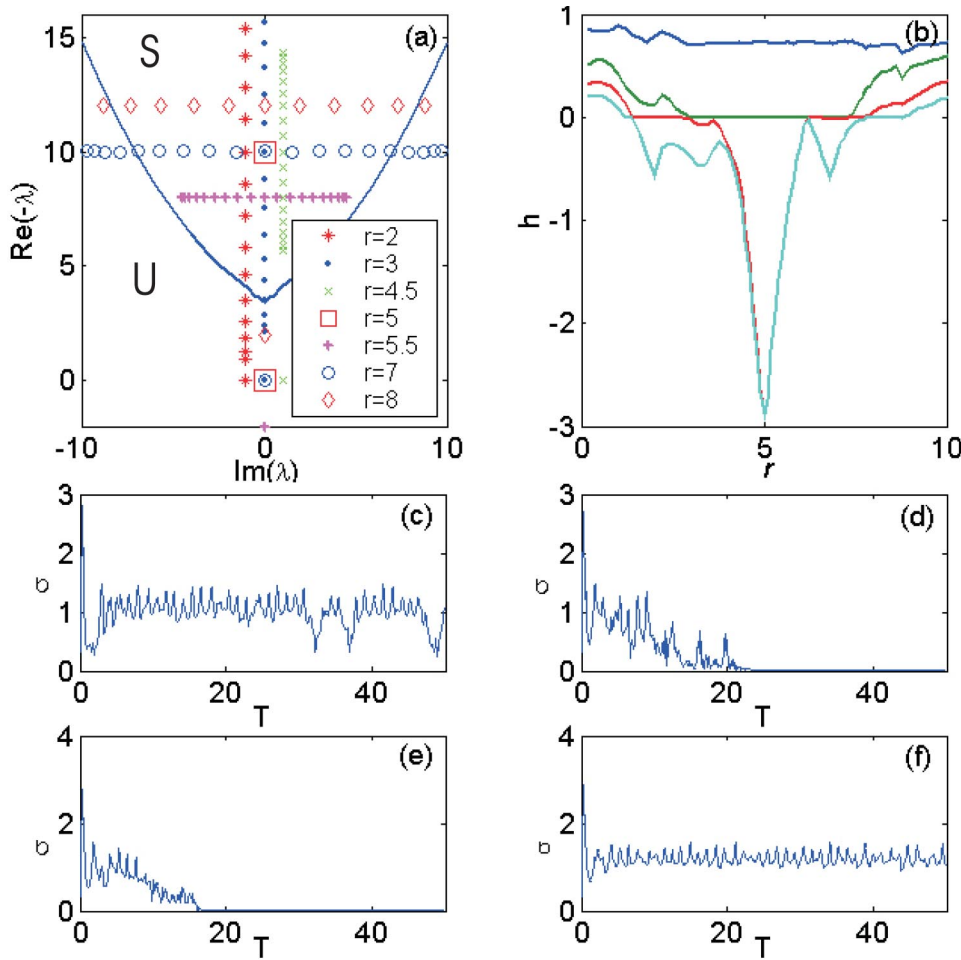


FIG. 2. (Color online) $N=20$ and $\epsilon=5$. (a) The eigenvalue distributions for various r . To make the picture clear, we shift the eigenvalues for the same r , for example, we move the eigenvalues upward by two units. The solid line is the critical curve which divides $\text{Re}(-\lambda)-\text{Im}(\lambda)$ parameter plane into stable (“S”) and unstable regions (“U”). (b) The four largest Lyapunov exponents vs the gradient coupling parameter r . (c)–(f) The evolution of the fluctuation defined in Eq. (9) for various r : (c) $r=2$; (d) $r=4.5$; (e) $r=5$; (f) $r=8$.

the location of the midpoint of the line. The competition between these two effects determines how the lowest eigenvalue moves along the line. Actually we find a diffusion coupling constant $\epsilon_c=r/\sin(k\pi/N)$ to be a turning point: the lowest eigenvalue on the line moves downward when $\epsilon < \epsilon_c$, otherwise it moves upward. As a result, for large ϵ a fourth critical ϵ_3 could be found, beyond which the distribution line moves back into the stable region and the synchronization is restored again. In Fig. 3(b), we show the four largest Lyapunov exponents versus ϵ . Two stable regions of the synchronous chaos are found. We also plot the time evolutions of σ in different parameter regimes [see Figs. 3(c)–3(h)]. The size effect on the synchronization is prominent in systems with PBC. If synchronization is realized for a system with a given N , it will break down when the size of the system increases above a certain value N_c . The explanation is given in Ref. [9]. Actually, for a V-type critical curve the synchronization requirement of ϵ and N for $r=0$ is

$$\epsilon(r=0) > \frac{|\lambda^*(0)|}{2[-1 + \cos(\frac{2\pi}{N})]}, \quad (10)$$

where $\lambda^*(0)$ can be read from the critical curve shown in Fig. 2(a) [23]. Similar results can be obtained for $r \neq 0$. The

numerical result for the relation of ϵ and N when $r=0$ is shown in Fig. 4(c) which is in great agreement with Eq. (10). However, the situation is quite different for the NBC case. We show the simulation results in Fig. 4(a) for $r \neq 0$. For small N , the situation is similar to the PBC case; there exists only one critical ϵ above which the synchronization is stable. However, when N is increased beyond a certain value N^* , an unstable region bursts out of the synchronization region from $(N^*, \epsilon^*) = (2\pi/\arcsin|\lambda^*(0)|/2r, 2r^2/|\lambda^*(0)|)$. The transitions between synchronization and desynchronization shown in Fig. 3 are clear in Fig. 4(a) when N is large. Up to this point, we have discussed the size effect on the synchronization. However, the phase diagram in the N - ϵ plane shown in Fig. 4(a) is different from that for the PBC case. Scrutinized in the stable region at small ϵ but large N , the boundary separating it from the desynchronization region is not sensitive to N [for example, see Fig. 4(b)]. The fact that the eigenvalue is $(N-1)$ -fold degenerate at $\epsilon=r$ hints that it is possible to find a regime where the stability of the synchronous chaos is independent of N . Such a regime in the ϵ - r plane can be obtained by $\sqrt{r^2 - |\lambda^*(-2\epsilon)|^2}/4 \leq \epsilon \leq (|\lambda^*(0)|^2 + 4r^2)/4|\lambda^*(0)|$ for $r \geq |\lambda^*(0)|/2$.

In summary, we have investigated the synchronization of coupled chaotic oscillators with no-flux boundary condition. We have found that the spectrum of the coupling matrix is divided into two parts, the isolated part with a zero eigenvalue and the continuous part with the other $N-1$ eigenval-

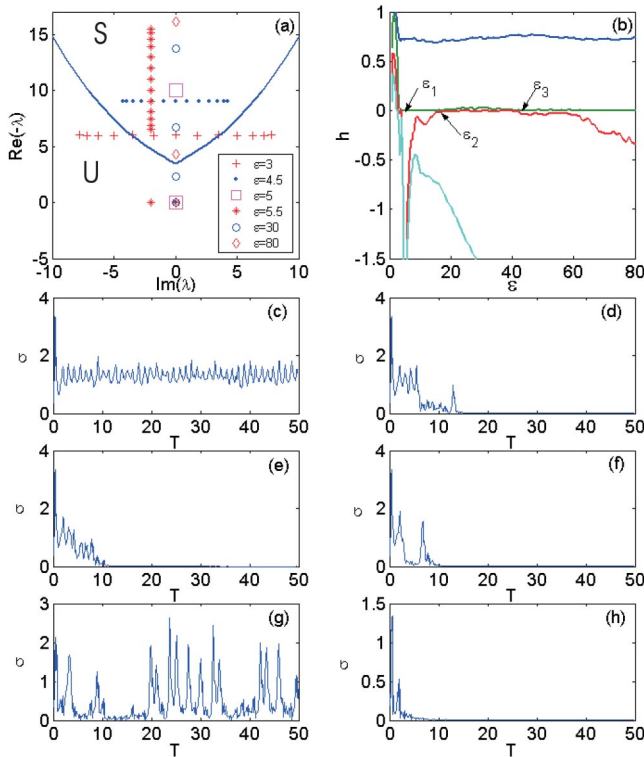


FIG. 3. (Color online) $N=14$, $r=5$. (a) The eigenvalue distributions for various ϵ . To see clearly, we shift the eigenvalues in the same way as Fig. 2. The solid line represents the critical curve. (b) The four largest Lyapunov exponents versus diffusive coupling parameter ϵ . (c)–(h) The evolution of the fluctuation for various ϵ : (c) $\epsilon=3$; (d) $\epsilon=4.5$; (e) $\epsilon=5$; (f) $\epsilon=5.5$; (g) $\epsilon=30$; (h) $\epsilon=60$.

ues falling onto a distribution line. The distribution line changes its orientation when diffusion coupling ϵ crosses the gradient coupling r . The midpoint of the distribution line is determined by the diffusion coupling while the width of the

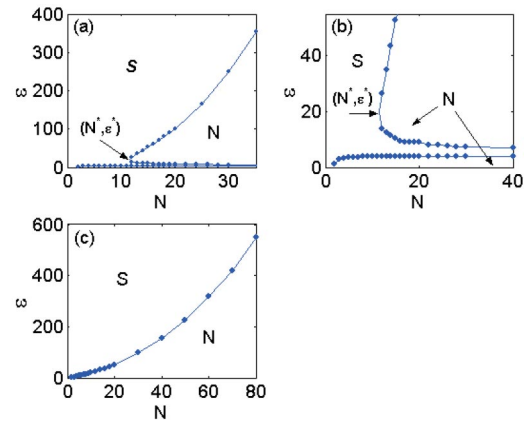


FIG. 4. (Color online) The phase diagram in the N - ϵ plane where the regime denoted by “N” (“S”) means desynchronization (synchronization). (a) The system with no-flux boundary condition. A new desynchronization region is born at (N^*, ϵ^*) . (b) The enlarged plot of (a) where $\epsilon < 50$. (c) The system with the periodic boundary condition.

line is dependent of the size of the system, the diffusion, and gradient coupling constant. Based on the eigenvalue analysis, the parameter space N - r - ϵ is explored. Numerical experiments on the coupled Lorenz systems with V-type critical curve are presented. Though our numerical discussion is made on a specific system, the results obtained in this paper can be extended to other systems. Since no-flux boundary condition is prevailing in natural systems such as the chemical reaction system, it is interesting to investigate the dynamical behavior caused by the peculiar property of the spectrum. The work along this line is still to be done.

This work was supported by Grant No. 10172020 from the Chinese Natural Science Foundation.

- [1] L. M. Pecora and T. L. Carroll, Phys. Rev. Lett. **64**, 821 (1990).
- [2] M. G. Rosenblum, A. S. Pikovsky, and J. Kurths, Phys. Rev. Lett. **76**, 1804 (1996).
- [3] A. S. Pikovsky, M. G. Rosenblum, G. V. Osipov, and J. Kurths, Physica D **104**, 219 (1997).
- [4] N. F. Rulkov, M. M. Sushchik, L. S. Tsimring, and H. Abarbanel, Phys. Rev. E **51**, 980 (1995).
- [5] L. Kocarev and U. Parlitz, Phys. Rev. Lett. **76**, 1816 (1996).
- [6] A. Maritan and J. R. Banavar, Phys. Rev. Lett. **72**, 1451 (1994).
- [7] D. He, P. Shi, and L. Stone, Phys. Rev. E **67**, 027201 (2003).
- [8] J. Yang, G. Hu, and J. Xiao, Phys. Rev. Lett. **80**, 496 (1998).
- [9] G. Hu, J. Yang, and W. Liu, Phys. Rev. E **58**, 4440 (1998).
- [10] L. M. Pecora and T. L. Carroll, Phys. Rev. Lett. **80**, 2109 (1998).
- [11] J. F. Heagy, L. M. Pecora, and T. L. Carroll, Phys. Rev. Lett. **74**, 4185 (1995).
- [12] J. F. Heagy, T. L. Carroll, and L. M. Pecora, Phys. Rev. Lett. **73**, 3528 (1994).
- [13] M. A. Matias, V. P. Munuzuri, M. N. Lorenzo, I. P. Marino, and V. P. Villar, Phys. Rev. Lett. **78**, 219 (1997).
- [14] G. Hu, J. Z. Yang, W. Q. Ma, and J. H. Xiao, Phys. Rev. Lett. **81**, 5314 (1998).
- [15] J. F. Heagy, T. L. Carroll, and L. M. Pecora, Phys. Rev. E **50**, 1874 (1994).
- [16] L. M. Pecora, Phys. Rev. E **58**, 347 (1998).
- [17] V. N. Belykh, I. V. Belykh, and M. Hasler, Phys. Rev. E **62**, 6332 (2000).
- [18] C. W. Wu and L. O. Chua, IEEE Trans. Circuits Syst., I: Fundam. Theory Appl. **43**, 161 (1996).
- [19] D. Armbruster and G. Dangelmayr, Math. Proc. Cambridge Philos. Soc. **101**, 167 (1987).
- [20] I. Epstein and M. Golubitsky, Chaos **3**, 1 (1993).
- [21] G. Hu, J. Xiao, J. Yang, F. Xieand, and Z. Qu, Phys. Rev. E **56**, 2738 (1997).
- [22] F. Willeboordse and K. Kaneko, Phys. Rev. Lett. **73**, 533 (1993).
- [23] $\lambda^*(0)$ is the eigenvalue where the critical curve intersects the $\text{Re}(-\lambda)$ axis. $\lambda^*(r)$ ($r \neq 0$) is the imaginary part of the eigenvalue where the critical line and $\text{Re}(-\lambda)=2\epsilon$ intersect.